

Orographic Vortex Shedding – Comparisons using Different Nested Grid Options in ARW WRF

JOHN LINDEMAN¹, ZAFER BOYBEYI
College of Sciences, George Mason University, Fairfax, VA
¹ author email: jlindema@gmu.edu

DAVE BROUTMAN
Computational Physics, Inc., Springfield, VA

Abstract

The Advanced Research WRF (ARW) model is used to investigate how orography of sufficient height affects the background atmospheric flow. In particular, an idealized case is chosen where mountain-generated shedding vortices propagate downstream and impact the lateral boundary. In this case, it is desirable to use nested grids because of (1) possible contamination by the lateral boundaries, and (2) the grid resolution can have an effect on the model solution. Results from several tests using one- and two-way nested grids are presented to determine how the inner nest is affected by the choice of nesting scheme. These results are then compared to a corresponding high resolution run of the same case on an area the size of the parent domain and another run using the inner nest area, but with an open lateral boundary condition.

1. Introduction

Mountains of a reasonable height can significantly distort the lower atmospheric airflow, causing nonlinearities in an initial unperturbed flow that can only be resolved by high-resolution numerical simulations. Examples of such nonlinearities include upstream flow blocking, airflow splitting around a mountain, hydraulic jump-like features over the lee slope which are sometimes associated with windstorms, valley flows, wake regions, and vortex generation. Vortex generation and shedding, which is examined here, are sometimes evident in cloud patterns captured by weather satellites (Figure 1).

The ARW WRF model was chosen to carry out this research as it has been thoroughly tested for linear and non-linear idealized cases involving orographic flows (Doyle, 2004). Schar and Durran (1997) analyzed shedding vortices with a three-dimensional non-linear model using an idealized

bell-shape mountain and an asymmetrical potential temperature perturbation.

Similar simulations with the WRF model using a nested grid are presented here. This particular case was chosen because the downstream lateral boundary is directly affected by the propagating vortices. This is a good sensitivity test of the 1-way and 2-way nesting schemes for the types of flows examined in my research. A high resolution run, on a domain the size of the parent domain, will serve as a control run.

In a 1-way nested scheme, the inner nest lateral boundaries come from their corresponding location on the parent domain. The 2-way nested scheme uses the same procedure as the 1-way nest for obtaining the inner nest lateral boundaries, but in addition the solution of the inner nest replaces the corresponding portion of the parent domain that lies spatially within the inner nest.

Clark and Farley (1984) compared 1-way and 2-way nesting schemes in their anelastic model for



Figure 1. NASA satellite photo of vortex shedding off of Guadalupe Island (June 2001).

resolution-dependant cases involving mountain waves. The 2-way nested scheme performed better than its 1-way nested counterpart, as phase velocities in the 1-way coarse mesh had errors that grew in time. Skamarock and Klemp (1993) applied 2-way nests for their adaptive mesh framework in a compressible model.

The next section describes the set-up of the WRF model experiments, the results of which are shown in section 3, and in section 4 the conclusions are presented.

2. Experimental Configuration

A total of four WRF model simulations are conducted. Two of them involve variations in the nested configuration of WRF, the third is a high-resolution simulation of an area the size of the parent domain, and the fourth simulation is for an area the size of the inner nested domain, but with open lateral boundary conditions. All cases use the non-hydrostatic version of ARL-WRF, 5th order horizontal advection and 3rd order vertical advection, the 1.5 order TKE closure scheme for K (calculated in physical space) is employed, and the 3rd order Runge-Kutta time step option with 6 acoustic time steps is used.

a. Model Run Configurations

Both nested model runs have one inner nest and a parent domain. The nest has 121 grid points in the x-direction (n_x), 76 grid points in the y-

direction (n_y), and a horizontal resolution of 650 m (delh). For the parent domain, $n_x=121$, $n_y=61$, and $\text{delh}=1950$ m. The relation of the inner nest to the parent domain can be seen in Figure 2. The parent domain has a time step of 5 s, and the inner domain has a time step one-third as large. The lateral boundary conditions of the outer domain are open (radiative).

Both of the non-nested high-resolution runs (where delh equals delh of the inner nest) use open (radiative) lateral boundary conditions. The control run has a domain the spatial size of the parent domain in the nested run, and the other run has a spatial domain the size of the inner nest.

All of the runs have 51 grid points in the vertical direction (n_z) and the top was set to 6150 m. The surface is free-slip, and the upper boundary employs a Rayleigh damping sponge layer beginning at 3 km to absorb upward propagating mountain waves.

It should be noted that this particular case does contain some vertical propagation of mountain waves. This is of concern, as downward wave reflection will occur off the upper boundary (or the sponge layer itself) if this layer is not sufficiently deep and does not contain enough grid points in the vertical direction. Following the analysis of Klemp and Lilly (1978), it has been determined that the sponge layer here is sufficient, as it contains 23 grid points and covers more than half of the vertical wavelength generated by the mountain.

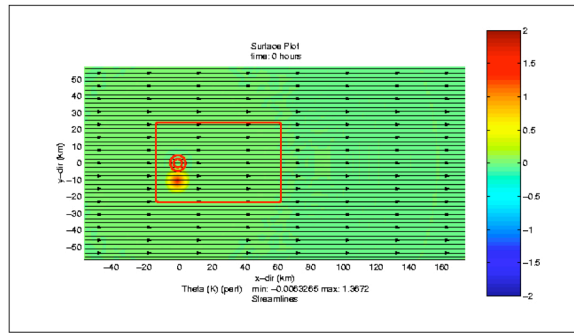


Figure 2. Surface regions of the parent domain and the inner nest (bounded by the red box). The 2 red circles show orographic contours at 500 m and 1 km, respectively, and the orange shaded circle is the initial potential temperature perturbation.

b. WRF Initialization

Both the inner nest and parent domain of the WRF model are initialized identically. A one-dimensional atmospheric profile is used to initialize WRF with a constant static stability $N = .01 \text{ s}^{-1}$, and initial wind speed $u = 5 \text{ ms}^{-1}$ ($v = 0 \text{ ms}^{-1}$). The Coriolis force is turned off for these simulations, and all runs are dry.

To generate the shedding vortices, a potential temperature perturbation is added to the initial conditions 8 km south of the mountain (see Figure 2). The perturbation is 8 km in diameter horizontally, extends 3 km in the vertical, has a surface maximum of 1.5 K, and decreases in magnitude linearly from its center.

The orography is initialized with the function:

$$h(i,j) = h_m / (1 + ((i-i_0)/a)^2 + ((j-j_0)/a)^2)^{3/2}$$

and is centered at $i_0 = 1/4$ and $j_0 = 1/2$ of the parent domain. $H_m = 1.5 \text{ km}$, and a , the mountain's half width at half-height, is 4 km. Orography from the parent domain is linearly interpolated to the inner nest.

All cases are run for 10 hours.

3. WRF Model Results

After 10 hours of simulation time, the lead vortices have propagated beyond the lateral boundary of the inner nest, but have not quite reached the edge of the parent domain.

Figures 3a and 3b show the inner grid for the 1-way and 2-way nests, respectively. Some differences exist in the location of the vortices between the two figures. These differences are most likely due to the fact that the inner nest lateral boundaries obtained from the outer domain are slightly different. These then can be compared with corresponding plots of the coarse parent domain (from the 1-way nested run) in Figure 4a, and the high-resolution simulation of the parent domain (Figure 4b). Differences in the location and intensity of the vortices can be attributed to the difference in horizontal resolution. The results from the inner nest area run with open lateral boundaries (Figure 4c) look altogether different. There is significant contamination from the open lateral boundaries, which are too close to the mountain forcing.

The importance of resolution in this case is exemplified by figures 3 and 4. The coarse resolution of the parent domain leads to inaccuracies in the inner nest. Choosing the best lateral boundary conditions possible is also very important for this type of simulation, as the entire inner nest is affected by the interaction of the propagating vortices and the lateral boundaries.

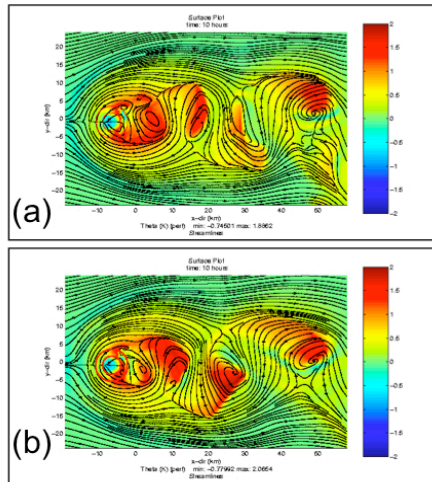


Figure 3. Inner nest surface plots of the potential temperature perturbation and horizontal streamlines for the (a) 1-way nest and (b) 2-way nest.

4. Conclusions

It is evident from these simulations that the 2-way nest run performs at least as well as the 1-way nest run, while the inner nest simulation with the open boundary conditions has an erroneous result due to the location of the lateral boundaries relative to the forcing (mountain). Thus for these simulations, those involving a nested grid yield the most accurate results.

A future test is planned to determine whether changing the location of the inner nest relative to the mountain can affect its accuracy (especially if the nest is moved upstream, so that its upstream lateral boundary is further from the mountain). It is hoped that this will yield more accurate results for the 2-way nested run.

Acknowledgments

I would like to thank Jun Ma for his assistance on configuring WRF, and Zafer Boybeyi, Dave Broutman, and Stephen Eckermann. This research is supported by the NSF.

5. References

Clark, T.L., and R.D. Farley, 1984: Severe downslope windstorm calculations in two and three spatial dimensions using anelastic interactive grid nesting: a possible mechanism for gustiness. *J. Atmos. Sci.*, **41**, 329-350.

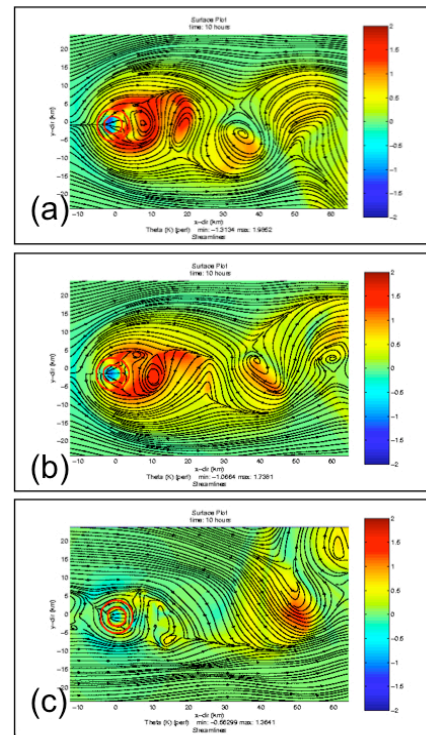


Figure 4. Same as Fig. 3, but corresponding to the inner region of (a) the coarse domain in the 1-way nested run, (b) the high resolution control run, and (c) the run with radiative lateral BC's.

Doyle, J.D., 2004. Evaluation of topographic flow simulations from COAMPS and WRF. *Proceedings, 16th Conference on Numerical Weather Prediction*, 11-15 Jan. 2004 Amer. Met. Soc., Seattle, WA, CD-ROM, 12.5.

Klemp, J.B., and D.K. Lilly, 1978: Numerical simulation of hydrostatic mountain waves. *J. Atmos. Sci.*, **35**, 78-107.

Schar, C. and D.R. Durran, 1997: Vortex formation and vortex shedding in continuously stratified flows past isolated topography. *J. Atmos. Sci.*, **54**, 534-554.

Skamarock, W.C., and J.C. Klemp, 1993: Adaptive Grid Refinement for two-dimensional and three-dimensional nonhydrostatic atmospheric flow. *Mon Weather Rev.*, **121**, 788-804.

Skamarock, W.C., Klemp, J.C., Dudhia, J., Gill, D.O., Barker, D.M., Wang, W., and J.G. Powers, 2005: A description of the advanced research WRF version 2. *NCAR Technical Note*, Boulder, CO, USA.